

PCCP

Accepted Manuscript



This is an *Accepted Manuscript*, which has been through the Royal Society of Chemistry peer review process and has been accepted for publication.

Accepted Manuscripts are published online shortly after acceptance, before technical editing, formatting and proof reading. Using this free service, authors can make their results available to the community, in citable form, before we publish the edited article. We will replace this *Accepted Manuscript* with the edited and formatted *Advance Article* as soon as it is available.

You can find more information about *Accepted Manuscripts* in the [Information for Authors](#).

Please note that technical editing may introduce minor changes to the text and/or graphics, which may alter content. The journal's standard [Terms & Conditions](#) and the [Ethical guidelines](#) still apply. In no event shall the Royal Society of Chemistry be held responsible for any errors or omissions in this *Accepted Manuscript* or any consequences arising from the use of any information it contains.

Intramolecular Hydrogen Bond Involving Organic Fluorine in the Derivatives of Hydrazides: An NMR Investigation substantiated by DFT based theoretical calculations

Cite this: DOI: 10.1039/x0xx00000x

Received 00th January 2012,
Accepted 00th January 2012

DOI: 10.1039/x0xx00000x

www.rsc.org/

Sandeep Kumar Mishra and N. Suryaprakash*

The rare examples of intramolecular Hydrogen bonds (HB) of the type the N–H•••F–C, detected in a low polarity solvent in the derivatives of hydrazides, by utilizing one and two-dimensional solution state multinuclear NMR techniques, are reported. The observation of through-space couplings, such as, $^1J_{FH}$, and $^1J_{FN}$, provides direct evidence for the existence of intra-molecular HB. Solvent induced perturbations and the variable temperature NMR experiments unambiguously establish the presence of intramolecular HB. The existence of multiple conformers in some of the investigated molecules is also revealed by two dimensional HOESY and ^{15}N - ^1H HSQC experiments. The ^1H DOSY experimental results discard any possibility of self or cross dimerization of the molecules. The derived NMR experimental results are further substantiated by Density Function Theory (DFT) based Non Covalent Interaction (NCI), and Quantum Theory of Atom in Molecule (QTAIM) calculations. The NCI calculations served as a very sensitive tool for detection of non-covalent interactions and also confirm the presence of bifurcated HBs.

Introduction

Hydrogen bonding is one of the most important non-covalent interactions in chemistry and biology¹⁻⁴. Numerous reports in past few decades lead to the availability of voluminous information on the self-assembly of molecules driven by HB⁵⁻¹⁷. Most of the reported intramolecular HB pertains to the motifs O•••H–N and N•••H–N¹⁸⁻²². The first nuclear magnetic resonance (NMR) spectroscopic observation of the involvement of organic fluorine in the HB in the solution state was reported by the detection of through space ($^1J_{FH}$) coupling²³. Subsequently the group of Limbach have

made enormous contributions to the growth of this field and reported several examples where not only organic fluorine but also the participation of other halogens in the intermolecular HB²⁴⁻²⁷. It is also well known that organofluorine molecules have enormous applications as drugs, agro chemicals, biomaterials and also in molecular imaging^{28, 29}. The organic fluorine has gained interest in the molecular association, such as, crystal engineering³⁰⁻³² and in the design of the functional materials³³. In bio-inorganic and medicinal chemistry, the formation of intermolecular X–H•••F–C (X=O, N) hydrogen bridges is significantly important because of the binding

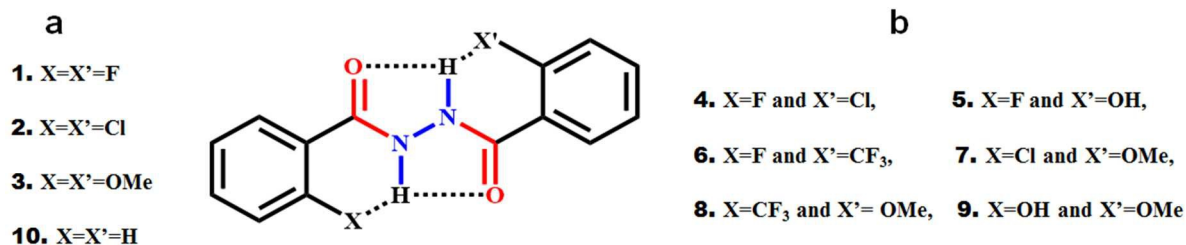
nature of the fluorinated compounds to enzyme active sites.³⁴⁻³⁸ In spite of the fact that fluorine containing organic molecules have great importance in number of fields, the study of intramolecular HB involving organic fluorine is limited owing to the fact it hardly ever accepts intramolecular HB^{39-43 44, 45}. This is also substantiated by a report of Dunitz and co-workers entitled “organic fluorine hardly ever accepts hydrogen bonds”⁴⁶⁻⁴⁹. However, there are very few reports of the involvement of organic fluorine in the HB in the solution state⁵⁰⁻⁵². The NMR and X-ray crystallographic studies on the N-H...F-C HB have been reported in foldamers and benzanilides^{53, 54}. Exclusive solution state NMR studies of the intramolecular HB of the type X-H...F-C (X=O, N) are reported on the derivatives of benzanilide and benzamide^{44, 45}. Hydrazides are organic compounds that share a common functional group with N-N covalent bond where at least one of the four substituents should be an acyl group⁵⁵. Different derivatives of hydrazides have proven to be extremely important as, reagents in organic synthesis,⁵⁶ anti-tumor medicine,^{57, 58} and also in the cytotoxic functioning⁵⁹. The derivatives of hydrazides are utilized in combination with other medicines for treatment or prevention of tuberculosis⁶⁰. The hydrazides also provide a possibility to synthesize variety of derivatives with the substitution of interested acyl group(s). In the present study many derivatives of hydrazides have been synthesized and characterized using one and two dimensional multinuclear NMR experiments, and ESI mass spectrometry. The procedure for synthesis of organic molecules and the relevant NMR spectra are reported in the supporting information. The NMR experiments reveal the existence of weak intramolecular interactions in all the investigated molecules. The NMR derived HB information has been

further substantiated by Density Function Theory (DFT)^{61, 62} based Non Covalent Interaction (NCI)⁶³, and Quantum Theory of Atom in Molecule (QTAIM)⁶⁴ calculations.

Results and discussion

NMR spectral parameter that provides information on the HB is the variation of chemical shift under different experimental conditions. Since the chemical shift is the consequence of electronic environment around the nuclei, the down field shift in the resonance frequency is observed for a proton which gets involved in HB consequent to the depletion of the electron density surrounding it. Number of NMR experiments are available to monitor the change in the chemical shift and to derive information on HB, viz., altering in the polarity of the solvent, changing the concentration of the solution (titrations experiments), and temperature induced perturbations. Another parameter that provides unambiguous evidence for the existence of HB is the detection of through space coupling between NMR active nuclei, where the transfer of spin polarization is mediated through hydrogen bond. The through space couplings can be determined using one and two dimensional homo- and hetero- nuclear correlation experiments. The ¹⁹F possessing ½ spin angular momentum is a favourable NMR active nucleus consequent to its 100% natural abundance. Thus one and two dimensional NMR experiments involving ¹⁹F have been carried out. In the present work the different possible derivatives of hydrazide, **1-10**, with generic name, 2-X-N-(2-X')benzohydrazide, whose basic chemical structures and their site specific substituents are given in scheme 1, have been investigated. The symmetrically disubstituted molecules are classified into two categories, one where X=X' (**1-3** and **10**) and the other where X≠X' (**4-9**).

ARTICLE



Scheme 1. The chemical structures of 2-X-N-(2-X')benzohydrazide derivatives.

There is a possibility that such molecules can undergo self or cross dimerization. The absence of any type of intermolecular dimerization of the studied molecules was confirmed by the 2D DOSY^{65, 66} experiments and ESI-MS analysis. The DOSY experiment was carried out for the mixture of molecules **1** and **3** (20 mM final solution) at the 1:1 molar ratio in solvent CDCl₃. The corresponding spectrum is given in Fig. 1.

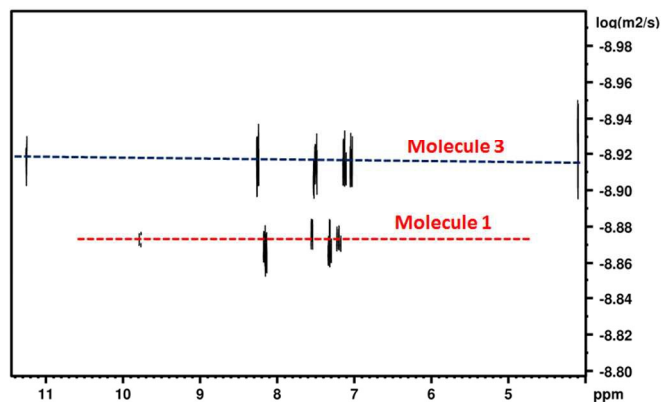


Figure 1. Two dimensional ¹H DOSY NMR spectrum of 20 mM solution of the mixture of molecules **1** and **3** at a 1:1 molar ratio in the solvent CDCl₃.

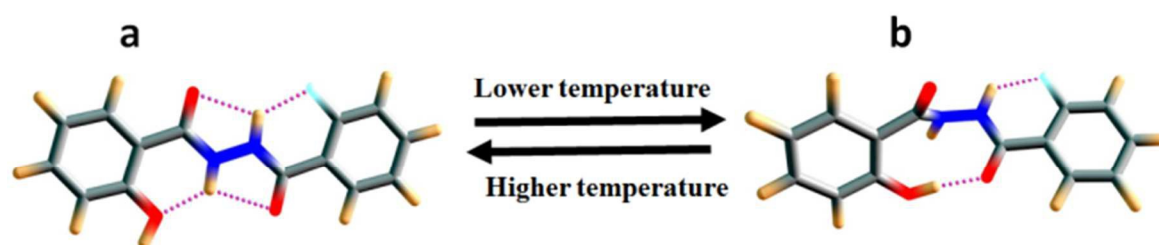
It is evident from Fig.1 that both the molecules exhibit different coefficients of diffusion. If there was a possibility of dimerization a single diffusion coefficient would have been measured for the mixture. The absence of dimerization may be attributed to the non-participation of

the bulky OMe group of the molecule **3** either in self or cross dimerization. On the other hand, the molecule **1** can get involved in self-dimerization. However, from Fig. 1 one can visualize that the diffusion rate of molecule **3** is slower than that of molecule **1**, thereby eliminating any possibility of its self-dimerization.

Solvent titration experiment^{50-52, 67} is employed to understand the weak interactions, such as, intra- and inter- molecular HB, to compare the relative strengths of interaction and also to evaluate the effect of monomeric water on HB, which is absorbed from atmosphere. Dilution studies has thus been carried out on the molecules **1-9** in the solvent CDCl₃, and the plot of the variation of chemical shift as a function of the solvent concentration is reported in Fig. 2(a). There is no significant effect of concentration is detected on the chemical shift of NH proton in the ¹H NMR spectra providing another strong evidence for the absence of any aggregation or dimerization due to intermolecular interaction. The chemical shift of the monomeric water in the CDCl₃ solvent that resonates at 1.54 ppm remained nearly constant with only marginal change of about 0.02 ppm during CDCl₃ titration indicating that it has no effect on the intramolecular HB⁶⁸. The lowering of temperature results in the strengthening of HB and causes excessive deshielding of proton due to displacement of NH proton towards the H-acceptor, providing strong evidence for the presence of HB⁶⁹⁻⁷¹. The variation in the chemical shift

of NH proton as a function of lowering of the temperature (300-220 K) is compared, for molecules 1-9, in Fig.2b. It is obvious from Fig. 2b that, except for molecule 5, the NH proton chemical shifts of all the molecules moved downfield due to the strengthening of HB at lower temperature. The unusual behaviour of the NH proton of the molecule 5 can be interpreted as due to its temperature dependent switching over of its two conformations. The possibility of such a switching phenomenon is illustrated in scheme 2. At lower temperature the molecule 5 is stabilized as a conformer where proton of OH is hydrogen bonded to

oxygen of CO group through a nine membered ring. As a result the NH proton, which is hydrogen bonded to OH group becomes weaker (scheme 2), and moves towards high field region (Fig. 2b). This is also confirmed by the gradual downfield shift of OH proton (11.31 ppm at 298 K) of the molecule 5, due to its involvement in the HB. The OH and NH peak positions reverted back to their original chemical shift positions on systematically increasing the temperature. This phenomenon further strengthens the stabilization of another conformer at lower temperature.



Scheme 2. Two different possible conformations of molecule 5, stable (a) at higher temperature, and (b) at lower temperature.

In the subsequent study we attempted to qualitatively derive the relative strengths of the intramolecular HBs, by titrating the solution with dimethyl sulphoxide (DMSO), since it is well known that DMSO is a very good HB acceptor. The observed variation in the chemical shifts as a function of the incremental addition of DMSO- d_6 is plotted for the molecules 1-9, in Fig. 2c. Disruption of intramolecular HB^{44, 45} by the solvent DMSO results in the deshielding of NH protons. On the contrary, for the molecules 3, 7, 8 and 9 high field shift of NH protons was detected. This is due to the fact that in these molecules HB

involving OMe group and NH proton is relatively stronger than the DMSO interaction and the high field shift of NH proton hydrogen bonded to OMe group is interpreted as an equilibrium which is stabilized between intra- and inter- molecular hydrogen bonded species. It is also evident from Fig. 2c that the proton H-bonded to F and OH groups resulted in high field shifts upto certain concentration of DMSO, and thereafter the downfield shift was detected due to the rupturing of intramolecular HB.

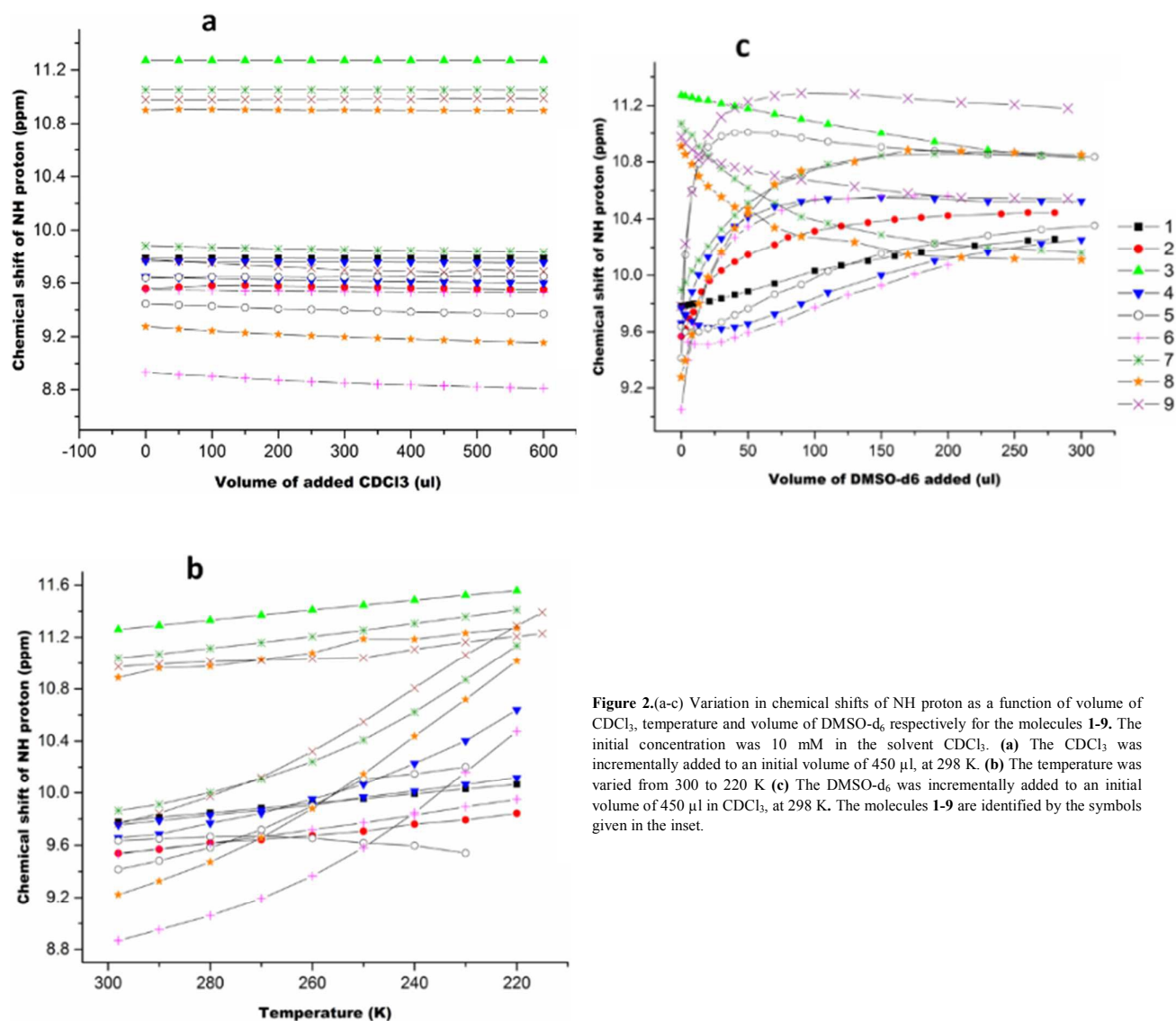


Figure 2.(a-c) Variation in chemical shifts of NH proton as a function of volume of CDCl₃, temperature and volume of DMSO-d₆ respectively for the molecules 1-9. The initial concentration was 10 mM in the solvent CDCl₃. (a) The CDCl₃ was incrementally added to an initial volume of 450 μl, at 298 K. (b) The temperature was varied from 300 to 220 K (c) The DMSO-d₆ was incrementally added to an initial volume of 450 μl in CDCl₃, at 298 K. The molecules 1-9 are identified by the symbols given in the inset.

ARTICLE

Table 1. The difference in the chemical shift of NH proton measured when the temperature is varied from 300 to 220 K, and from lower to higher concentrations of solvents CDCl₃ and DMSO, for the molecules **1-9**. The $^1J_{NH}$ was measured in the solvent CDCl₃. The $^1J_{NH}$ of -98.23 Hz was measured for the molecule **10** in the solvent CDCl₃.

Molecule	Proton involved in HB with (X...HN)	Change in chemical shift (ppm)			$^1J_{NH}$ in the solvent CDCl ₃
		On adding 600 μ l CDCl ₃	On adding 300 μ l DMSO	Temperature varied from 300 to 220 K	
1	(F...HN)	-0.0010	0.4748	0.2869	-102.78
2	(Cl...HN)	-0.0081	0.8760	0.3027	-100.76
3	(MeO...HN)	+0.0003	-0.4275	0.2984	-103.18
4	(F...HN)	-0.0119	0.4835	0.36383	-103.61
	(Cl...HN)	-0.0479	0.8624	0.9821	-102.33
5	(F...HN)	+0.0097	1.4193	0.7848	-101.37
	(HO...HN)	-0.0920	0.7165	-0.0943	-98.76
6	(F...HN)	-0.0176	0.5041	0.6077	-102.06
	(CF ₃ ...HN)	-0.1207	1.5109	0.4151	-101.21
7	(Cl...HN)	-0.0028	0.9333	1.27245	-101.66
	(MeO...HN)	-0.0477	0.0866	0.37045	-102.45

8	(MeO...HN)	-0.0025	-0.7987	0.3832	-103.90
	(CF ₃ ...HN)	-0.1203	1.5729	1.79355	-102.26
9	(MeO...NH)	+0.0097	-0.4326	0.2569	-102.83
	(HO...NH)	-0.0920	1.3998	1.62855	-101.20

Another interesting NMR parameter that provides very useful information about HB is the detection of couplings between two NMR active nuclei involved in hydrogen bond, where the spin polarization is transferred across the hydrogen bond⁷²⁻⁷⁵. The ¹⁹F coupled and decoupled ¹H spectrum of molecule **1** in the solvent CDCl₃, and the ¹⁹F coupled spectrum in the solvent DMSO-d₆ are given in Fig. 3. The NH peak of the molecule **1** is a doublet with a separation of 12.75 Hz (Fig. 3a). It may be pointed out that the NH peak in Fig. 3a appears like a quartet, which is due to the presence of both ^{2h}J_{FN} and ^{1h}J_{FH}. This will become clear from the HSQC spectrum, discussed in the later part of the manuscript. The doublet collapses into a singlet in the ¹H⁴⁵ experiment confirming the presence of coupling between ¹H and ¹⁹F (Fig. 3c). Such a large value of the coupling mediated through covalent bond (³J_{FH}) between ¹H and ¹⁹F is very unlikely^{44, 45} and might be mediated through HB (^{1h}J_{FH}). This is ascertained by recording the spectrum in a high polarity solvent DMSO-d₆ instead of CDCl₃, which resulted in the collapsing of doublet to a singlet (Fig.3b).

ARTICLE

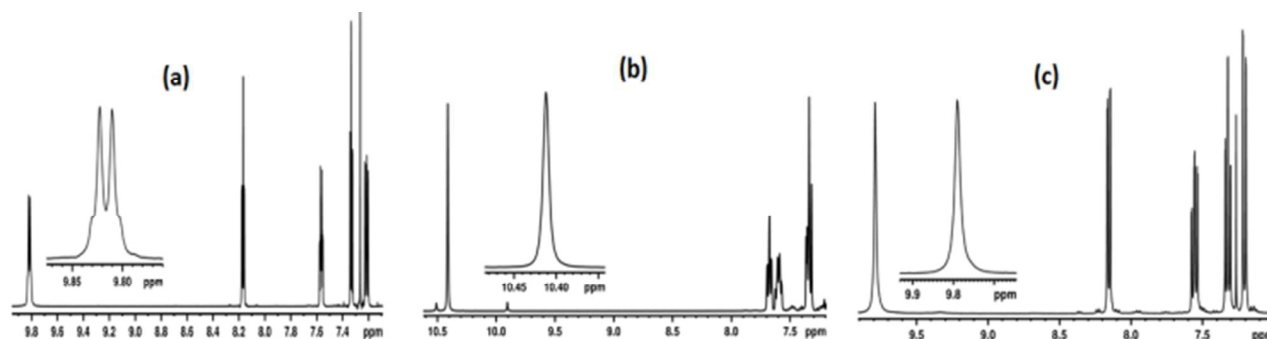


Figure 3: 400 MHz ^1H NMR spectrum of molecule **1**; (a) in the solvent CDCl_3 ; (b) ^1H NMR spectrum in solvent DMSO-d_6 and (c) $^1\text{H}\{^{19}\text{F}\}$ NMR spectrum in solvent CDCl_3 .

However, the $^3J_{\text{HH}}$ and $^4J_{\text{FH}}$ couplings, if any, are not detectable due to the symmetry of the molecule. For the determination of these values, which provides another strong evidence for the existence of HB, we resorted to the technique of extracting the coupling among equivalent spins by breaking the symmetry of the molecule. For such a purpose we have carried out the two dimensional proton-coupled ^1H - ^{15}N HSQC experiment for the molecule **1**, where ^{15}N is present in its natural abundance and the corresponding spectrum is reported in Fig. 4(A). In the isotopomer with a single ^{15}N at natural abundance, there is a possibility of detecting, all the seven couplings, $^1J_{\text{NH}}$, $^2J_{\text{FN}}$, $^2J_{\text{NH}}$, $^3J_{\text{FN}}$, $^1J_{\text{FH}}$, $^4J_{\text{FH}}$ and $^3J_{\text{HH}}$. The measurable couplings from both the ^1H and ^{15}N dimensions of HSQC spectrum are marked with alphabets and their values are reported in the figure. The observation of through space couplings of significant strengths, such as $^1J_{\text{FH}}$, $^2J_{\text{FN}}$, $^3J_{\text{FN}}$ and $^4J_{\text{FH}}$,

gives strong and direct evidence for the involvement of organic fluorine in the intramolecular HB. The NH-coupled ^1H - ^{15}N HSQC experiment in the solvent DMSO-d_6 was also carried out and the corresponding spectrum is given in Fig. 4(C). In the solvent DMSO , except for $^1J_{\text{NH}}$, all the other couplings mediated through hydrogen bond disappeared. This gives the unambiguous evidence that the measured couplings $^1J_{\text{FH}}$, $^2J_{\text{FN}}$, $^3J_{\text{FN}}$ and $^4J_{\text{FH}}$ in the solvent CDCl_3 are mediated through HB. One of the through bond couplings $^3J_{\text{HH}}$ could not be determined from the HSQC spectrum in the solvent DMSO . The ^1H - ^{15}N HSQC spectra of all the other investigated molecules, along with the measured coupling values are reported in supporting information.

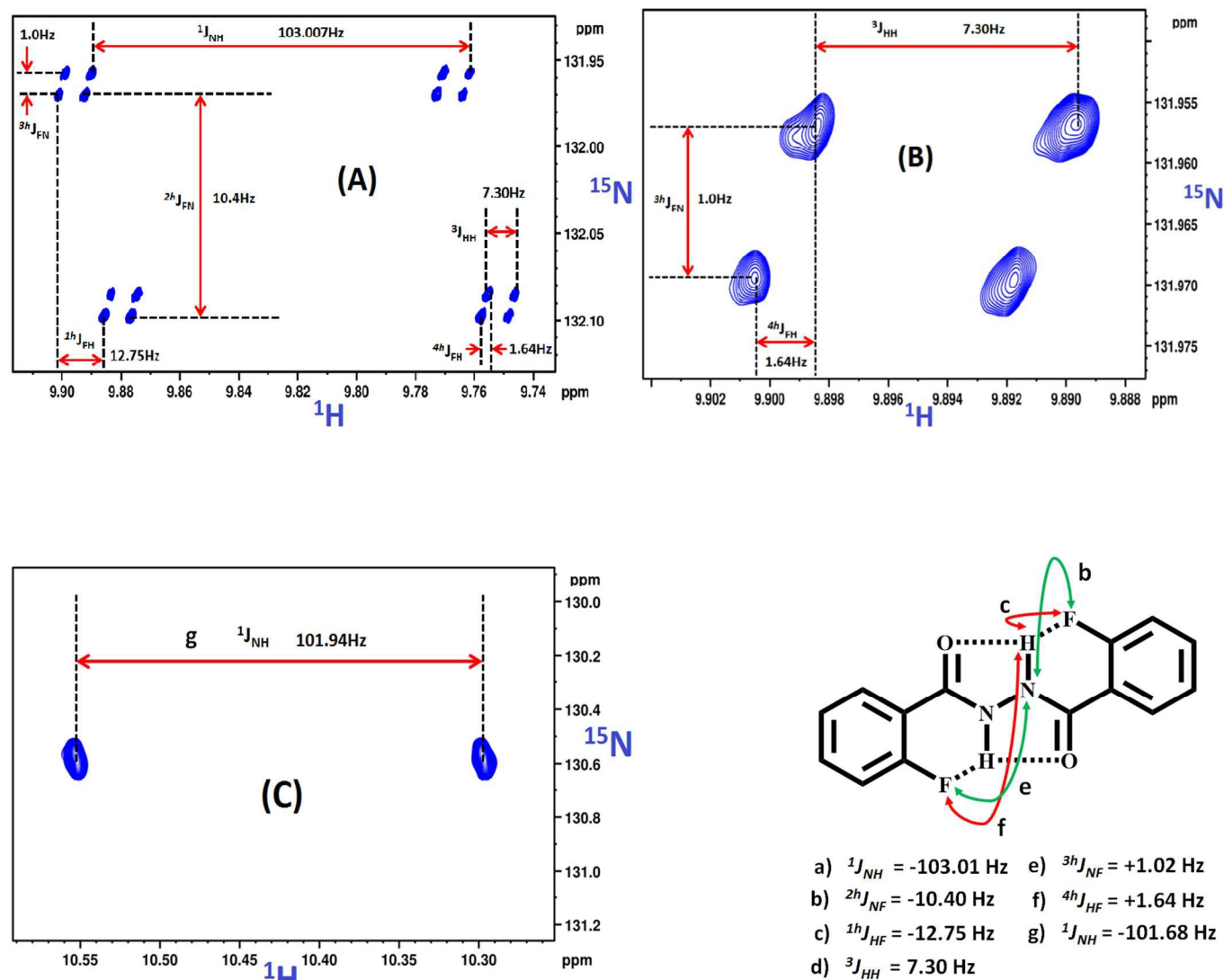


Figure 4. (A) 800 MHz ^1H - ^{15}N -HSQC (NH-coupled) spectrum of molecule **1** in the solvent CDCl_3 ; (B) Expanded region enclosed in the green box in Fig.4(A); (C) 400 MHz ^1H - ^{15}N -HSQC spectrum (NH-coupled) in the solvent DMSO-d_6 . The molecular structure and the separations that gives magnitudes of scalar and through space couplings are identified by double headed arrows. The measured coupling values are their signs derived from the relative slopes of displacement of cross sections are also given.

From Figs. 4(A) and 4(B) the magnitudes and relative signs of the couplings could be derived. Assuming $^1J_{\text{FH}}$ (marked as c) to be negative as reported earlier^{44, 45} the relative slopes of the displacement of cross sections indicate that sign of $^4J_{\text{FH}}$ (marked as f) is positive. Similarly $^2J_{\text{FN}}$ (marked as b) is reported to be negative, then from the slope of the displacement cross sections the sign of $^3J_{\text{FN}}$ (marked as e) is determined

to be positive. All the measured magnitudes of the couplings along with their appropriate signs are given in the figure.

The value of $^1J_{\text{NH}}$ has a great significance as far as the nature of HB is concerned. If HB is predominantly electrostatic then its strength increases⁷⁶ and if the HB is predominantly a covalent type its strength

decreases⁷⁷. Thus the NH coupled ^{15}N - ^1H HSQC experiments were carried out for all the investigated molecules in the solvent CDCl_3 and the measured couplings are compiled in Table 1. The visual comparison of these values with $^1J_{\text{NH}}$ coupling (-98.23Hz) of an unsubstituted molecule **10**, it can be inferred that the $^1J_{\text{NH}}$ couplings of the substituted molecules **1-9** are substantially smaller than the molecule **10**, providing ample evidence that the nature of HBs in derivatives of hydrazides are predominantly covalent.

The change in the intensity of peak in nuclear Overhauser effect spectrum is correlated to the spatial proximity between two spins

involved in dipolar interaction. Hence nuclear Overhauser (nOe) effect can be exploited to correlate the strength of HB in the molecule. Thus the 2D ^1H - ^{19}F hetero nOe spectroscopy (HOESY)⁷⁸⁻⁸⁰ experiments, where the through space correlation is established between NH proton and the F atom in the molecules, have been carried out for all the fluorine containing molecules. The 2D ^1H - ^{19}F HOESY spectrum of the molecule **1** is reported in the Fig. 5. The HOESY spectra of molecules, **4**, **5**, **6**, and **8** are reported in ESI. The strong correlation between F and NH proton is an indication of close spatial proximity between F and NH proton which favors the existence of intramolecular HB.

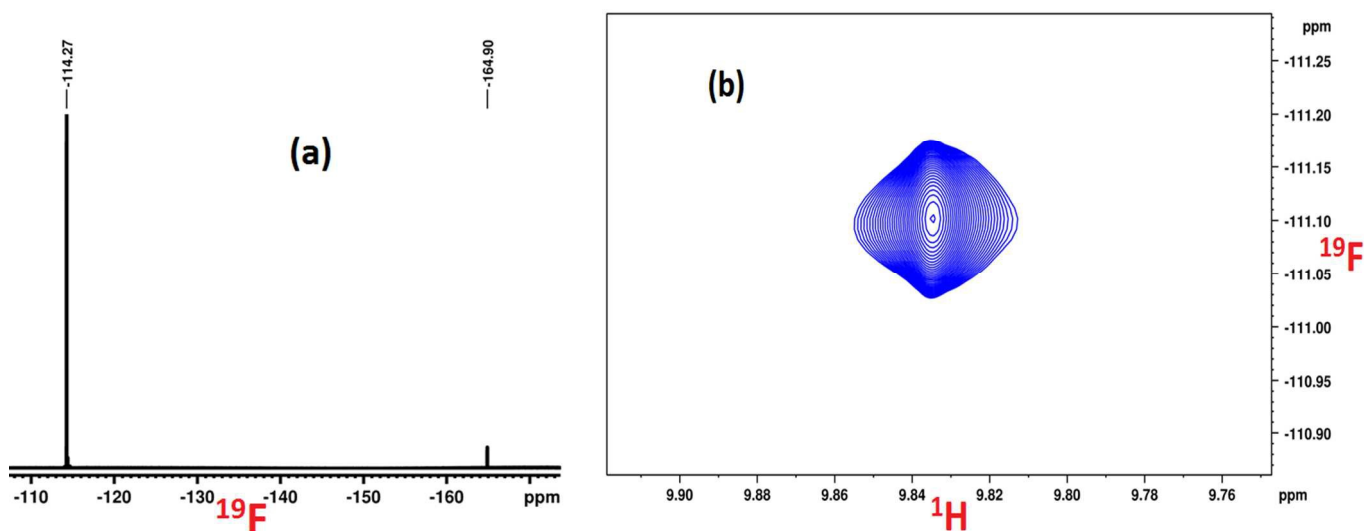


Figure 5. (a) ^{19}F and (b) 2D ^1H - ^{19}F HOESY spectra of the molecule **1** acquired using 400 MHz NMR spectrometer in the solvent CDCl_3 . The hexafluorobenzene (C_6F_6), ^{19}F chemical shift of -164.90 ppm is used as internal reference for all the ^{19}F spectra.

The various NMR experiments carried out on all the investigated molecules provided strong evidence for the involvement of organic fluorine in HB.

Theoretical calculations

The weak molecular interactions established by NMR studies were also corroborated by theoretical DFT^{61, 62} optimized structure based calculations. The DFT calculations were performed using Gaussian09

suit,⁸¹ with B3LYP/6-311+g (d,p) level of theory with the solvation medium (Default-chloroform) to optimize the lowest energy structures for all the investigated molecules **1-9**. The energy minimized structures were confirmed by harmonic vibrational frequency. The optimized molecular geometries were used to generate the wave function files for QTAIM, and NCI studies. The same optimized coordinates with identical parameters are used with CSGT⁹⁰ method for simulation of ¹H NMR spectra.

NCI plot

The non covalent interaction (NCI)⁸² theoretical approach is used to detect non-covalent interactions in real space, based on the electron density and its derivatives. It provides a rich representation of van der Waals interactions, HBs, and the steric repulsion. In density tails (i.e., regions far from the molecule, where the electron density exponentially

decays to zero), the reduced density gradient (RDG) will have very large positive gradient, and the RDG values will be small and approaches zero. This happens for the regions of both covalent and non-covalent bonding. In the corresponding region for the weak interactions having large correlation with electron density ($\rho(r)$), the correlations for the steric effect is negative and for the HB is positive. The van der Waals interaction will always have very small $\rho(r)$ values⁸². The calculated grid points are plotted for a defined real space function, $\text{sign}(\lambda_2(r))\rho(r)$, as function 1 and reduced density gradient (RDG) as function 2 using Multiwfn⁸³ program for the molecules **1-9**. The color filled isosurfaces have been plotted using these grid points by program VMD⁸⁴. The plot for the $\text{sign}(\lambda_2(r))\rho(r)$ v/s RDG, and the colored isosurfaces for the molecule **1** are reported in Figs. **5a** and **5b** respectively.

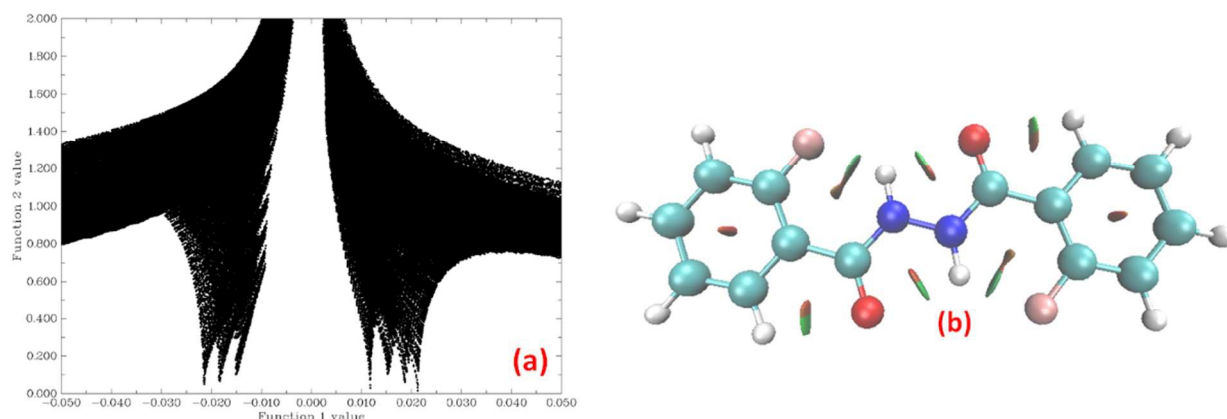


Figure 6. (a) The plot of $\text{sign}(\lambda_2(r))\rho(r)$ as function 1 v/s the RDG as function 2, and (b) coloured isosurface plot (green color denotes weak H-bond and red color stands for steric effect) for molecule **1**. The plots for remaining molecules, **2-8** are given in the supporting information.

There are three spikes on the left hand side of Fig.6a (i.e. $\text{sign}(\lambda_2(r))\rho(r)$ is negative) for the molecule **1** denoting three HBs, viz., N-H...F, N-H...O and C-H...O. These three HBs can be observed in Fig. 6b as

green coloured isosurfaces. The red colour in isosurface plot (Fig.6b) represents the steric hindrance arising from phenyl ring of the molecule and other HB mediated rings. This is seen as four spikes on the right

hand side (i.e. $\text{sign}(\lambda_2(r)) \cdot \rho(r)$ is positive) of Fig.6a. The similar plots for the molecules 2-8 are discussed in the supporting information.

method of NMR simulation. The given chemical shifts (ppm) are for the molecules 1-9 in solvent CDCl_3 . The chemical shift of NH proton at 9.23 ppm was measured for the molecule 10 in the solvent CDCl_3 .

Atoms in molecules (AIM) calculations

In addition to confirming the presence of HB by NCI plot, for in depth understanding of the molecular properties influenced by weak HBs, the information about the energy of interaction must be known. The topology analysis technique initially reported as "atoms in molecules" (AIM) theory, which is also cited as "the quantum theory of atoms in molecules" (QTAIM)^{64, 85-88} relies on quantum observables such as the electron density $\rho(r)$ and the energy densities. In topology analysis, the points where gradient norm of function value is zero (except at infinity) are called as critical points (CPs). CPs can be classified into four types according to the negative Eigenvalues of Hessian matrix of real space function^{64, 85-88}. Out of all four CPs, (3,-1) is commonly called as bond critical point (BCP). The value of real space function at BCP has great significance. For example the value of electron density $\rho(r)$ and the sign of Laplacian of electron density ($\nabla^2 \rho(r)$) at BCP are closely related to bond strength and bond type respectively^{64, 85-88}. The magnitudes of $\rho(r)$ and signs of $\nabla^2 \rho(r)$ for BCP of HBs of interest, calculated using QTAIM calculations, are compiled in Table 2. The potential energy density ($V(r)$) at corresponding (3, -1) critical points (r_{cp}) where the gradients of electron density ($\rho(r)$) get vanished, is directly related to the energy of HB (E_{HB}) by straightforward relationship⁸⁹ $E_{\text{HB}} = V(r_{\text{bcp}})/2$. The above discussed relationship is applicable to calculate the E_{HB} of $\text{X} \cdots \text{HX}$ type HB⁸⁹. The calculated values of E_{HB} for all the studied molecules at located BCPs are assimilated in Table 2.

Molecule	HB type (X...HN)	Electron density ($\rho(r)$) (a.u.)	Laplacian of electron density ($\nabla^2 \rho(r)$)	Energy of HB (E_{HB}) (Kcal/mol)	Theoretical CS of NH proton (ppm)	Experimental CS of NH proton (ppm)
1	(F...HN)	0.0215	0.0935	-5.6964	9.75	9.79
2	(Cl...HN)	0.0224	0.0764	-4.6865	9.70	9.56
3	(MeO...HN)	0.0292	0.1226	-7.7411	10.5	11.27
4	(F...HN)	0.0218	0.0949	-5.7828	9.3	9.76
	(Cl...HN)	0.0227	0.0770	-4.7620	9.1	9.65
5a	(F...HN)	0.0218	0.0944	-5.7686	9.4	9.78
	(HO...HN)	0.0267	0.1163	-6.8456	10.3	10.98
5b	(F...HN)	0.0228	0.0973	-6.0952	8.9	---
	(HO...HN)	0.0137	0.0561	-3.0533	8.5	---
	(OH...O)	0.0333	0.1113	-8.5621	---	---
6	(F...HN)	0.0216	0.0939	-5.7183	9.8	9.93
	(CF ₃ ...HN)	0.0141	0.0559	-3.3642	9.6	9.55
7	(Cl...HN)	0.0118	0.0455	-2.2735	10.6	9.88
	(MeO...HN)	0.0292	0.1218	-7.7411	11.5	11.05
8	(MeO...HN)	0.0283	0.1191	-7.3975	10.4	10.90
	(CF ₃ ...HN)	0.0171	0.0689	-4.2437	9.4	9.28
9	(MeO...NH)	0.0290	0.1217	-7.6618	10.4	10.98
	(HO...NH)	0.0266	0.1163	-6.8521	10.3	9.78

Table 2. Electron density ($\rho(r)$) and Laplacian of electron density ($\nabla^2 \rho(r)$) at different BCPs of type (3, -1) for (X...HN) H-bond. The energy of particular H-bonds calculated on the basis of potential energy density ($V(r)$) using formulae discussed above are also listed. The calculations were done using solvation medium of default-chloroform. Theoretically simulated chemical shift(ppm) of NH protons are calculated using CSGT

The bond paths and BCPs at the HB for all the molecules are reported in ESI. Such large values of $\rho(r)$ (Table 2) indicates the presence of significant interactions at (3,-1) BCPs. The sign of $(\nabla^2\rho(r))$ at BCP is having significance in discriminating the shared-shell (covalent bond (-ve)) and closed-shell (van der Waals interaction, ionic interactions and HB (+ve)). From Table 2 it is confirmed that, BCPs are coming under closed-shell (HB) interactions. The calculated strengths of HBs are compared with the chemical shifts of NH protons in Table 2. It is evident that the strength of HB is showing a direct correlation with chemical shift of NH (H-bonded) proton (downfield shift with increasing strength or *vice versa*). Thus by utilizing the E_{HB} or NMR chemical shifts in identical conditions we could compare the relative strengths of HBs. In addition to this the ^1H NMR spectra were simulated using GIAO⁹⁰ and CSGT⁹⁰ methods of NMR simulation. NMR studies confirmed that some of the molecules exist in more than one conformation. Hence the calculated chemical shift values of NH protons deviated slightly from the experimental data. The values observed from CSGT method are almost comparable with the experimental results given in Table 2.

Experimental

The NMR spectra were recorded for all the investigated molecules using Bruker AVANCE 400, 500 and 800 MHz NMR spectrometers. Proton chemical shifts are measured with TMS as internal reference (TMS, 0.0 ppm). All the ^{19}F spectra were referenced to internal hexafluorobenzene. For characterization of synthesized molecules, all the NMR spectra were acquired at 298 K (except for the temperature dependent studies). Deuterated solvents, such as, CDCl_3 , and $\text{DMSO-}d_6$ were purchased from Cambridge Isotopes Limited and used as received. In general the strength of non-covalent interactions are found to be dependent on solvent and substrate purity. Thus fresh CDCl_3 was used to avoid the possibility of artificial alteration in the interaction strength. Electrospray ionization mass spectrometric data was collected (ESI-MS) to confirm molecular mass of the synthesized molecules. The two dimensional HSQC, HOESY and DOSY spectra were acquired using the standard programs available in the software library of Bruker NMR spectrometers.

General procedure for synthesis of hydrazides

Different substituted hydrazides were synthesized using the corresponding benzoyl chlorides. All benzoyl chlorides, and concentrated hydrazine hydrate ($\text{NH}_2\text{NH}_2\cdot\text{H}_2\text{O}$) of high purity were purchased from Sigma Aldrich and used as received. The AR grade solvent methylene chloride (CH_2Cl_2), chloroform (CHCl_3) and n-pentane (C_5H_{12}) were used in the synthesis. To the best of our knowledge this method for synthesis of hydrazides is not reported and this is the first report.

Step 1: Synthesis of unsubstituted hydrazides (R-CONH₂NH₂)

200 mgs of benzoyl chloride was kept in an ice bath in a ml round bottom flask (RB) and cooled to 0°C. The cooled 1.1-equivalent concentrated $\text{NH}_2\text{NH}_2\cdot\text{H}_2\text{O}$ in 1 ml CD_2Cl_2 was added drop by drop using dropping funnel with continuous stirring of the reaction mixture. A precipitate was formed during this process. After complete addition of hydrazine hydrate the ice bath was removed and the reaction mixture was stirred at room temperature for 2 minutes. Then the solvent CH_2Cl_2 was added to the RB containing reaction mixture and shaken till the precipitate gets completely dissolved. Subsequently the 50 ml of distilled water was added to this solution. A biphasic mixture of two solutions thus obtained was transferred to the separating funnel and was separated out from each other. The solvent CH_2Cl_2 was evaporated using a rotatory evaporator at the temperature and pressure of 45°C and 500 mm Hg respectively. White crude compound left in RB was dissolved in 5 ml chloroform and was kept overnight for crystallization with addition of 0.1 ml of methanol. The ^1H NMR spectra were recorded for characterization. The ^1H NMR spectra and ESI MS analysis of all the compounds gave evidence for the pure form of the synthesized compound.

Step 2: Synthesis of N-substituted hydrazides (R-CONH-NH-R')

The benzoyl chloride of interest was kept at 0°C in ice bath, and to this 0.9 equivalents of cooled compound synthesized as discussed in the step 1 was added drop by drop using dropping funnel. Then the procedure similar to step 1 was repeated. Some impurity peaks were seen in the region of 1-1.5 ppm in the ^1H NMR spectrum. For further purification, the compounds were washed with n-pentane three times and then dried for complete evaporation of n-pentane. This washed compound was analyzed using ^1H , ^{13}C NMR and electrospray ionization mass spectrometry (ESI-MS) and the formation of expected hydrazides was confirmed.

Conclusions

The combined NMR experimental observations and DFT based theoretical calculations revealed the existence of intramolecular HBs in different derivatives of hydrazides. The existence of more than one conformers are established in several molecules by using different NMR studies. CDCl₃ concentration titration and ¹H DOSY technique are utilized to discard any possibility of self or cross dimerization. The ¹H-¹⁹F HOESY experiment is utilized to extract the information about the possibility of intramolecular HB by through space correlation, as well as for the determination of different conformers. Through space coupling via HB is detected by 2D ¹H-¹⁵N HSQC, experiment, whose magnitudes varied between 1-14 Hz in several F-containing molecules. The NCI calculations acted as a very sensitive tool for detection of non-covalent interactions, also confirm the presence of bifurcated HBs in the molecules **1-9**. To derive the energy of HBs, the QTAIM calculations are utilized and the strengths of different HBs present in investigated molecules are calculated to be in the range of -2.27 to -9.62 kcal/mol.

The Laplacian of electron density sign is used to discriminate the HBs from the covalent bonds. We believe that the present studies might lead to better understanding of the HB and open up opportunities in designing of different foldamers and supramolecules that are of chemical and biological importance.

Acknowledgements

SKM would like to thank UGC, New Delhi, for SRF. Authors thank Prof. T.N. Guru Row and Sounak Sarkar for fruitful discussions on theoretical calculations. NS gratefully acknowledges the generous financial supported by Board of Research in Nuclear Sciences, Mumbai (Grant No. 2013/37C/4/BRNS) and the Science and Engineering Research Board, Department of Science and Technology, New Delhi (grant No. SR/S1/PC-42/2011)..

Notes and references

Mr. Sandeep Kumar Mishra and Prof. N. Suryaprakash
NMR Research Centre, Solid State and Structural Chemistry Unit,
Indian Institute of Science,
Bangalore-560012 (INDIA)
Tel: 00918022933300; Fax: +918023601550
E-mail: nsp@nrc.iisc.ernet.in

Electronic Supplementary Information (ESI) available: [details of any supplementary information available should be included here]. See DOI: 10.1039/b000000x/

References

1. W.-H. Hu, K.-W. Huang, C.-W. Chiou and S.-W. Kuo, *Macromolecules*, 2012, 45, 9020-9028.
2. M. Saccone, V. Dichiarante, A. Forni, A. Goulet-Hanssens, G. Cavallo, J. Vapaavuori, G. Terraneo, C. J. Barrett, G. Resnati, P. Metrangolo and A. Priimagi, *J. Mater. Chem. C*, 2015, 3, 759-768.
3. A. J. P. Teunissen, M. M. L. Nieuwenhuizen, F. Rodriguez-Llansola, A. R. A. Palmans and E. W. Meijer, *Macromolecules*, 2014, 47, 8429-8436.
4. T. Xiao, X. Feng, S. Ye, Y. Guan, S.-L. Li, Q. Wang, Y. Ji, D. Zhu, X. Hu, C. Lin, Y. Pan and L. Wang, *Macromolecules*, 2012, 45, 9585-9594.
5. A. Ajayaghosh, S. J. George and A. P. H. J. Schenning, in *Top. Curr. Chem.* ed. F. Würthner, Springer Berlin Heidelberg, 2005, 258, 135681, 83-118.
6. E. A. Archer, H. Gong and M. J. Krische, *Tetrahedron*, 2001, 57, 1139-1159.
7. L. Brunsveld, B. J. B. Folmer, E. W. Meijer and R. P. Sijbesma, *Chem. Rev.* 2001, 101, 4071-4098.
8. M. M. Conn and J. Rebek, *Chem. Rev.* 1997, 97, 1647-1668.
9. F. Huang and H. W. Gibson, *Prog. Polym. Sci.* 2005, 30, 982-1018.
10. D. S. Lawrence, T. Jiang and M. Levett, *Chem. Rev.* 1995, 95, 2229-2260.
11. O. Lukin and F. Vögtle, *Angew. Chem., Int. Ed.* 2005, 44, 1456-1477.
12. J. S. Nowick, *Acc. Chem. Res.* 1999, 32, 287-296.
13. L. J. Prins, D. N. Reinhoudt and P. Timmerman, *Angew. Chem., Int. Ed.* 2001, 40, 2382-2426.
14. C. Schmuck and W. Wienand, *Angew. Chem., Int. Ed.* 2001, 40, 4363-4369.
15. R. Shenhar and V. M. Rotello, *Acc. Chem. Res.* 2003, 36, 549-561.
16. R. P. Sijbesma and E. W. Meijer, *Chem. Commun.* 2003, DOI: 10.1039/B205873C, 5-16.
17. F. Zeng and S. C. Zimmerman, *Chem. Rev.* 1997, 97, 1681-1712.
18. B. Gong, *Chem. Eur. J.* 2001, 7, 4336-4342.
19. I. Huc, *Eur. J. Org. Chem.* 2004, 2004, 17-29.
20. Z.-T. Li, J.-L. Hou, C. Li and H.-P. Yi, *Chem. Asian J.* 2006, 1, 766-778.
21. J. W. Lockman, N. M. Paul and J. R. Parquette, *Prog. Polym. Sci.* 2005, 30, 423-452.
22. A. R. Sanford, K. Yamato, X. Yang, L. Yuan, Y. Han and B. Gong, *Eur. J. Biochem.* 2004, 271, 1416-1425.

23. I. D. Rae, J. A. Weigold, R. H. Contreras and R. R. Biekofsky, *Magn. Reson. Chem.* 1993, 31, 836-840.
24. H. Benedict, I. G. Shenderovich, O. L. Malkina, V. G. Malkin, G. S. Denisov, N. S. Golubev and H.-H. Limbach, *J. Am. Chem. Soc.* 2000, 122, 1979-1988.
25. N. S. Golubev, I. G. Shenderovich, S. N. Smirnov, G. S. Denisov and H.-H. Limbach, *Chem. Eur. J.* 1999, 5, 492-497.
26. I. G. Shenderovich, S. N. Smirnov, G. S. Denisov, V. A. Gindin, N. S. Golubev, A. Dunger, R. Reibke, S. Kirpekar, O. L. Malkina and H.-H. Limbach, *Phys. Chem.* 1998, 102, 422-428.
27. I. G. Shenderovich, P. M. Tolstoy, N. S. Golubev, S. N. Smirnov, G. S. Denisov and H.-H. Limbach, *J. Am. Chem. Soc.* 2003, 125, 11710-11720.
28. I. Muegge, S. L. Heald and D. Brittelli, *J. Med. Chem.* 2001, 44, 1841-1846.
29. B. E. Smart, *J. Fluorine Chem.* 2001, 109, 3-11.
30. D. Chopra and T. N. G. Row, *CrystEngComm*, 2011, 13, 2175-2186.
31. G. R. Desiraju, *J. Am. Chem. Soc.* 2013, 135, 9952-9967.
32. K. Reichenbacher, H. I. Suss and J. Hulliger, *Chem. Soc. Rev.* 2005, 34, 22-30.
33. R. Berger, G. Resnati, P. Metrangolo, E. Weber and J. Hulliger, *Chem. Soc. Rev.* 2011, 40, 3496-3508.
34. R. H. Abeles and T. A. Alston, *J. Biol. Chem.* 1990, 265, 16705-16708.
35. M.-C. Chapeau and P. A. Frey, *J. Org. Chem.* 1994, 59, 6994-6998.
36. T. Kovacs, A. Pabuccuoglu, K. Lesiak and P. F. Torrence, *Bioorg. Chem.* 1993, 21, 192-208.
37. D. O'Hagan and H. S. Rzepa, *Chem. Commun.* 1997, DOI: 10.1039/A604140J, 645-652.
38. L. H. Takahashi, R. Radhakrishnan, R. E. Rosenfield, E. F. Meyer and D. A. Trainor, *J. Am. Chem. Soc.* 1989, 111, 3368-3374.
39. R. Banerjee, G. R. Desiraju, R. Mondal and J. A. K. Howard, *Chem. Eur. J.* 2004, 10, 3373-3383.
40. C. Li, S.-F. Ren, J.-L. Hou, H.-P. Yi, S.-Z. Zhu, X.-K. Jiang and Z.-T. Li, *Angew. Chem., Int. Ed.* 2005, 44, 5725-5729.
41. Y. Mido and T. Okuno, *J. Mol. Struct.* 1982, 82, 29-34.
42. H. Takemura, N. Kon, M. Yasutake, S. Nakashima, T. Shinmyozu and T. Inazu, *Chem. Eur. J.* 2000, 6, 2334-2337.
43. X. Zhao, X.-Z. Wang, X.-K. Jiang, Y.-Q. Chen, Z.-T. Li and G.-J. Chen, *J. Am. Chem. Soc.* 2003, 125, 15128-15139.
44. K. Divya, S. Hebbar and N. Suryaprakash, *Chem. Phys. Lett.* 2012, 525-526, 129-133.
45. G. N. Manjunatha Reddy, M. V. Vasantha Kumar, T. N. Guru Row and N. Suryaprakash, *Phys. Chem. Chem. Phys.* 2010, 12, 13232-13237.
46. D. Chopra, *Cryst. Growth Des.* 2011, 12, 541-546.
47. J. D. Dunitz, *ChemBioChem*, 2004, 5, 614-621.
48. J. D. Dunitz and R. Taylor, *Chem. Eur. J.* 1997, 3, 89-98.
49. J. A. K. Howard, V. J. Hoy, D. O'Hagan and G. T. Smith, *Tetrahedron*, 1996, 52, 12613-12622.
50. I. Alkorta, J. Elguero, H.-H. Limbach, I. G. Shenderovich and T. Winkler, *Magn. Reson. Chem.* 2009, 47, 585-592.
51. C. Bartolome, P. Espinet and J. M. Martin-Alvarez, *Chem. Commun.* 2007, DOI: 10.1039/B710304B, 4384-4386.
52. S. R. Chaudhari, S. Mogurampelly and N. Suryaprakash, *J. Phys. Chem. B*, 2013, 117, 1123-1129.
53. I. E. Kareev, G. S. Quiñones, I. V. Kuvychko, P. A. Khavrel, I. N. Ioffe, I. V. Goldt, S. F. Lebedkin, K. Seppelt, S. H. Strauss and O. V. Boltalina, *J. Am. Chem. Soc.* 2005, 127, 11497-11504.
54. G. K. S. Prakash, F. Wang, M. Rahm, J. Shen, C. Ni, R. Haiges and G. A. Olah, *Angew. Chem., Int. Ed.* 2011, 50, 11761-11764.
55. IUPAC, *Compendium of Chemical Terminology*, 2nd ed. (The "Gold Book"). Online corrected version: (2006-) "Hydrazides" 1997.
56. L. Friedman, R. L. Litle, and W. R. Reichle *Org. Synth.* 1960, 40, 93-96.
57. R. M. Mohareb, D. H. Fleita and O. K. Sakka, *Molecules*, 2010, 16, 16-27.
58. W. W. Wadrakhan, N. N. E. El-saeed, and R. M. Mohereb, *Acta Pharm.* 2013, 63, 45-57.
59. Z. Swietlińska and J. Žuk, *Mutation Res./Rev. Gen. Toxicology* 1978, 55, 15-30.
60. Z. A. Kaplancikli, G. Turan-Zitouni, A. Ozdemir and J.-C. Teulade, *Archiv der Pharmazie*, 2008, 341, 721-724.
61. W. Kohn and L. J. Sham, *Phys. Rev.* 1965, 140, A1133-A1138.
62. R.G. Parr and W. Yang, *Density-Functional Theory of Atoms and Molecules*, Oxford University Press, New York, 1989.
63. J. Contreras-García, W. Yang and E. R. Johnson, *J. Phys. Chem. A*, 2011, 115, 12983-12990.
64. R. F. W. Bader, *Atoms in Molecules: A Quantum Theory*, Oxford University Press, Oxford, 1990.
65. K. F. Morris and C. S. Johnson, *J. Am. Chem. Soc.* 1992, 114, 3139-3141.
66. K. F. Morris and C. S. Johnson, *J. Am. Chem. Soc.* 1993, 115, 4291-4299.
67. A. E. Reed, L. A. Curtiss and F. Weinhold, *Chem. Rev.* 1988, 88, 899-926.
68. M. Nakahara and C. Wakai, *Chem. Lett.* 1992, 21, 809-812.
69. S. H. Gellman, B. R. Adams and G. P. Dado, *J. Am. Chem. Soc.* 1990, 112, 460-461.
70. S. H. Gellman, G. P. Dado, G. B. Liang and B. R. Adams, *J. Am. Chem. Soc.* 1991, 113, 1164-1173.
71. F. J. Martinez-Martinez, A. Ariza-Castolo, H. Tlahuext, M. Tlahuextl and R. Contreras, *J. Chem. Soc., Perkin Trans. 2*, 1993, DOI: 10.1039/P29930001481, 1481-1485.
72. T. Axenrod, P. S. Pregosin, M. J. Wieder, E. D. Becker, R. B. Bradley and G. W. A. Milne, *J. Am. Chem. Soc.* 1971, 93, 6536-6541.
73. A. J. Dingley, J. E. Masse, R. D. Peterson, M. Barfield, J. Feigon and S. Grzesiek, *J. Am. Chem. Soc.* 1999, 121, 6019-6027.
74. A. Dunger, H.-H. Limbach and K. Weisz, *J. Am. Chem. Soc.* 2000, 122, 10109-10114.
75. S. Grzesiek, F. Cordier, V. Jaravine and M. Barfield, *Prog. Nucl. Magn. Reson. Spectrosc.* 2004, 45, 275-300.
76. A. V. Afonin, I. A. Ushakov, L. N. Sobenina, Z. V. Stepanova, O. g. V. Petrova and B. A. Trofimov, *Magn. Reson. Chem.* 2006, 44, 59-65.
77. M. M. King, H. J. C. Yeh and G. O. Dudek, *Org. Magn. Reson.* 1976, 8, 208-212.
78. P. L. Rinaldi, *J. Am. Chem. Soc.* 1983, 105, 5167-5168.
79. C. Yu and G. C. Levy, *J. Am. Chem. Soc.* 1983, 105, 6994-6996.
80. C. Yu and G. C. Levy, *J. Am. Chem. Soc.* 1984, 106, 6533-6537.
81. M. J. Frisch, G. W. Trucks, H. B. Schlegel, G. E. Scuseria, M. A. Robb, J. R. Cheeseman, G. Scalmani, V. Barone, B. Mennucci, G. A. Petersson, H. Nakatsuji, M. Caricato, X. Li, H. P. Hratchian, A. F. Izmaylov, J. Bloino, G. Zheng, J. L. Sonnenberg, M. Hada, M. Ehara, K. Toyota, R. Fukuda, J. Hasegawa, M. Ishida, T. Nakajima, Y. Honda, O. Kitao, H. Nakai, T. Vreven, J. A. Montgomery Jr., J. E. Peralta, F. Ogliaro, M. J. Bearpark, J. Heyd, E. N. Brothers, K. N. Kudin, V. N. Staroverov, R. Kobayashi, J. Normand, K. Raghavachari, A. P. Rendell, J. C. Burant, S. S. Iyengar, J. Tomasi, M. Cossi, N. Rega, N. J. Millam, M. Klene, J. E. Knox, J. B. Cross, V. Bakken, C. Adamo, J. Jaramillo, R. Gomperts, R. E. Stratmann, O. Yazyev, A. J. Austin, R.

- Cammi, C. Pomelli, J. W. Ochterski, R. L. Martin, K. Morokuma, V. G. Zakrzewski, G. A. Voth, P. Salvador, J. J. Dannenberg, S. Dapprich, A. D. Daniels, Ö. Farkas, J. B. Foresman, J. V. Ortiz, J. Cioslowski and D. J. Fox, Gaussian, Inc., Wallingford, CT, USA, 2009.
82. E. R. Johnson, S. Keinan, P. Mori-Sánchez, J. Contreras-García, A. J. Cohen and W. Yang, *J. Am. Chem. Soc.* 2010, 132, 6498-6506.
83. T. Lu and F. Chen, *J. Comput. Chem.* 2012, 33, 580-592.
84. W. Humphrey, A. Dalke and K. Schulten, *J. Molec. Graphics* 1996, 14, 33-38.
85. R. F. W. Bader, S. G. Anderson and A. J. Duke, *J. Am. Chem. Soc.* 1979, 101, 1389-1395.
86. R. F. W. Bader and H. Essén, *J. Chem. Phys.* 1984, 80, 1943-1960.
87. R. F. W. Bader, T. T. Nguyen-Dang, and Y. Tal, *Rep. Prog. Phys.* 1981, 44, 893-948;
88. G. R. Runtz, R. F. W. Bader and R. R. Messer, *Can. J. Chem.* 1977, 55, 3040-3045.
89. E. Espinosa, E. Molins and C. Lecomte, *Chem. Phys. Lett.* 1998, 285, 170-173.
90. J. R. Cheeseman, G. W. Trucks, T. A. Keith, and M. J. Frisch, *J. Chem. Phys.* 1996, 104, 5497-5509.

